JAM CM Journal of Applied Mathematics and Computational Mechanics 2024, 23(3), 31-42
www.amcm.pcz.pl p-ISSN 2299-9965
DOI: 10.17512/jamcm.2024.3.03 e-ISSN 2353-0588

PROGRESSIVE DESIGN OF THE TAKE-UP BAR WITHIN THE JET WEAVING MACHINE FOR THE PRODUCTION OF 3D FABRICS

Tomáš Koňařík[1], Karel Ráž[2]

[1] Department of Weaving Technology, VÚTS, a.s.
Liberec, Czech Republic
[2] Faculty of Mechanical Engineering, University of West Bohemia
Plzeň, Czech Republic
tomas.konarik@vuts.cz, kraz@fst.zcu.cz

Received: 6 August 2024; Accepted: 11 September 2024

Abstract. On the DIFA II loom, which is a special air jet weaving machine for the production of drop-stitch fabrics with a variable distance, so called 3D or distance fabrics, the main component of the interconnecting yarn creation mechanism is a take-up bar. During the yarn loops formation, the take-up bar is exposed to high loads, while being pulled by a mechanism into a limited wedge-shaped space between the two plain weave faces, thus the bending stiffness of the bar is crucial. Deflection of the bar combined with an elongation of the warp yarns results in an uneven load distribution with an undesirably loosened central section of warp yarns. This phenomenon is deeply examined in this paper. The classical model of a thin beam loaded by a distributed linear force cannot be applied in this case. In this work are new take-up bar designs considering usage and production aspects. The take-up bar variants with different warp yarns stiffness were analysed. A numerical model was created, and calculations were performed by the FEM solver NX Nastran as a 1D solution. Additionally, the problem was analysed analytically and it shows an analogy with a beam on an elastic foundation. The theoretical Winkler's model was used and an idealised analytical solution was found. In both methods, comparable maximal deflections of the take-up bar and widths of loosened yarns were found. The obtained results of the bar deflection were validated with a good agreement on the DIFA II loom using new take-up bars.

MSC 2010: *34A99, 65L99*
Keywords: *weaving machine, drop-stitch, FEM simulation, Winkler's model*

1. Introduction

In the technical textile sector, various spatial textile structures have been looked into recently [1]. The demand for drop-stitch fabric (knitted or woven) is growing, especially for the production of inflatable objects, but not solely; the applicability is wide. Current weaving or knitting machines are limited by their production processes and can only produce drop-stitch fabric at a certain constant distance. The uniqueness

of the DIFA II weaving machine lies in the fact that it can produce high-strength drop-stitch fabric with a variable distance in the direction of the warp yarns and can process coarse and even very fine yarns.

In Figure 1, a distance fabric weaving mechanism is illustrated [2]. The interconnecting pile yarns are formed in the discontinuous weaving sequence with lateral removal of the take-up bar every few seconds. The take-up bar, as a crucial component, enters into an open shed, then is grasped by electromagnets. There are blocks of magnets, arranged in a Halbach array [3], mounted in the take-up bar endings, shown in Figure 3. Then the bar is pulled between two plain weave fabrics by the distance L, which defines the final drop-stitch fabric distance (from 100 mm up to 500 mm). The take-up bar, by its move, drags a pile of yarns. Due to the comparatively similar bending stiffness of the bar and the tensile stiffness of the yarns, the deflection of the bar causes uneven tension in interconnecting yarns, actually loosening the yarns in the central section, which may affect the final product quality.

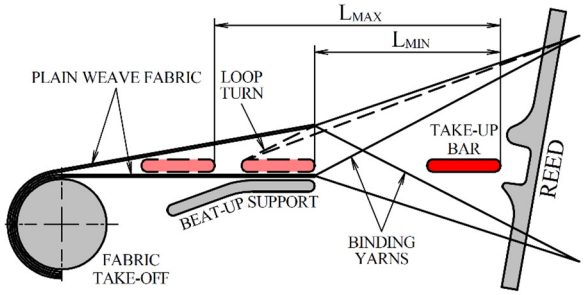

Fig. 1. A 3D fabric weaving mechanism. The fabric distance is defined by the take-up bar travel in the range between L_{MIN} and L_{MAX}

These quality issues are not visible in the raw 3D fabric and are not a problem in some applications, but in the case of double-sided coated inflatable products, there may appear noticeably uneven patterns from binding yarns.

The behaviour of the whole system is dependent on material and mechanical properties of binding yarns and the number of yarns in the warp systems. Unfortunately, there is high variability in those properties due to the universality of the DIFA II machine, allowing to produce 3D fabrics in a wide specification range.

2. The take-up bar designs

Due to the specific take-up bar function, working cycle, and manipulation area, there are key desired properties considered in its design: low and narrow profile; high bending stiffness; lightweight; non-magnetic; low friction coefficient; surface hardness, wear resistance, etc. The take-up bars' front endings, in the direction of entering into a shed, are tilted and rounded (Figs. 3 and 18) due to smooth insertion. The rear bar's endings are rounded with double-sided chamfered grooves (Figs. 4 and

18), which are used for the attachment to tweezers of the manipulation mechanism. Furthermore, the bar endings are provided with tapered holes used for positioning the bar in the open shed, and also for detaching the bar from electromagnets via tapered pins.

Originally the DIFA I weaving machine used a take-up bar profile illustrated in Figure 2a. Despite certain qualities, the bar was costly, complicated to manufacture, and the main issue was with a wavy surface after gluing the 0.15 mm thin metal sheet bends around the carbon composite core (Fig. 4). The initial net width of the distance fabric was 1.5 m, which corresponds to the needed bar length of 1.7 m. With demand to lower the 3D fabric distance and increase its width to 2 m (the bar length of 2.2 m), a next narrower bar design (Fig. 2d) was introduced in the framework of upgrading to the DIFA II weaving machine. Much was resolved, however, the bending stiffness decreased significantly, which had a major effect on a fabric quality due to distinctively loosened binding yarns in the bar central area. Subsequently, several other designs, shown in Figure 2b, c, e, f, were proposed with certain improvements and trade-offs.

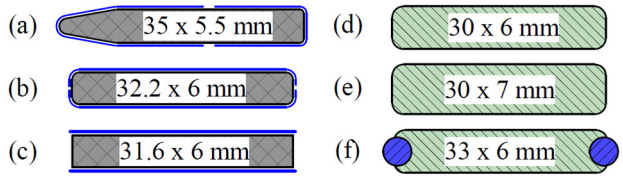

Fig. 2. Cross-sections of different variants of the take-up bar: a, b) stainless steel sheet bends glued on a carbon composite core; c) stainless steel plain sheet glued on a carbon composite core; d, e) anodized duralumin; f) anodized duralumin with glued stainless steel rods

In Table 1, some of the profile characteristics are listed, where the bending stiffness is crucial. Another important property is the weight of the bar, because the bar manipulation sequence time limits the production performance of the machine, therefore, a lighter bar allowing better dynamics is highly desirable.

Table 1. Profile characteristics of different take-up bar variants

Type	Bending stiffness EJ [Nm^2]	EJ compared to bar type a	Profile length weight [gm^{-1}]
a	1937	100 %	345
b	2031	105 %	515
c	1934	100 %	532
d	938	48 %	498
e	1100	57 %	582
f	1761	91 %	650

Fig. 3. The take-up bar (type c) stainless steel front ending with a block of magnets arranged in a Halbach array (state before assembling)

Fig. 4. Take-up bar rear ending, the original type a. The shading shows the problematic wavy surface after gluing the assembly

3. Analysis of the take-up bar

3.1. FEM simulations

The definition of the simulation model is illustrated in Figure 5. CAD model and calculations were performed by SW Siemens NX by employing the FEM solver NX Nastran as a 1D solution.

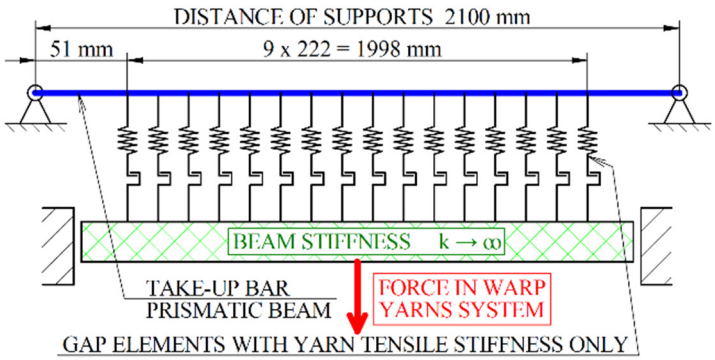

Fig. 5. Scheme of the simulation model

The definition of components and boundary conditions of the computational model is shown in Figures 6-11 (each relevant component is denoted by an orange colour) with respective descriptions.

The take-up bar is created using 1D elements of the BEAM type. The size of each element is 3 mm. The cross-section corresponds to the cross-sectional characteristic of the given profile with the respective material.

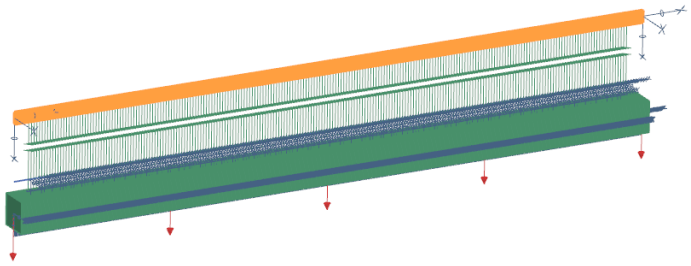

Fig. 6. FEM model definition – take-up bar

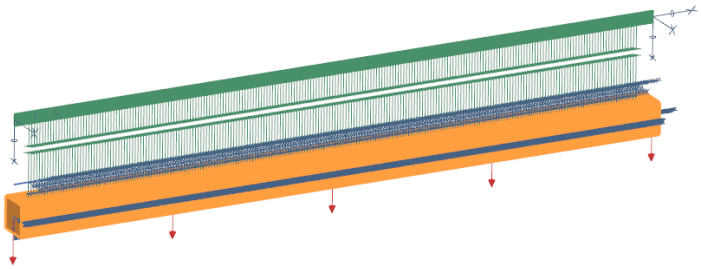

Fig. 7. FEM model definition – auxiliary beam

The auxiliary beam is used to apply load force to it and to hold the springs/gaps. It is a geometry from 1D elements of the BEAM type. Its stiffness is several orders of magnitude higher than that of the take-up bar. The material of the auxiliary beam is steel with a theoretical cross-section of 100×100 mm.

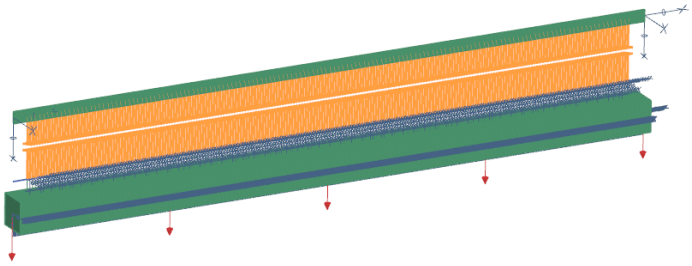

Fig. 8. FEM model definition – binding yarns

Binding yarns are replaced by 1D elements of the CGAP type in the number of 223 pieces. These elements have different definable stiffness in compression and tension. This approach is also used in [4], and it represents the behaviour of yarns. A stiffness of 420 Nm^{-1} for the first run, 840 Nm^{-1} for the second run, the tensile load of the element is considered. A negligible stiffness of $1 \cdot 10^{-10}$ Nm^{-1} is considered for the compressive load.

The attachment of the take-up bar is implemented by using a boundary condition fixing 5 out of 6 degrees of freedom. Only the rotation around the "z" axis is allowed. The distance of supports was set to 2100 mm, which is the pitch of the manipulation electromagnets.

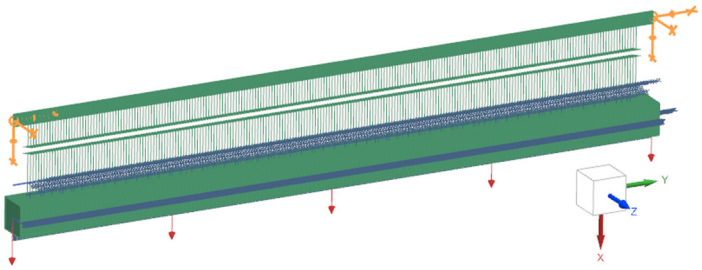

Fig. 9. FEM model definition – take-up bar attachment

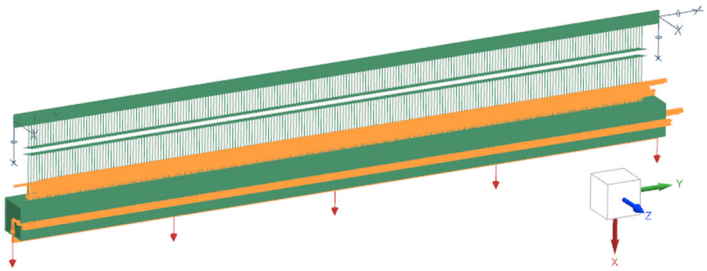

Fig. 10. FEM model definition – auxiliary beam stabilization

In order to stabilize the task, the boundary condition allowing only the displacement in the direction of the "x" axis was applied to the auxiliary beam. The other degrees of freedom were fixed.

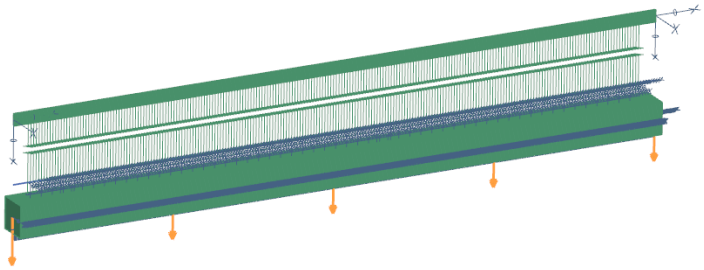

Fig. 11. FEM model definition – load force

The load force is applied to the auxiliary beam. In this case, the overall force is considered, in contrast to the control system of the weaving machine, where the force in the warp is usually related to the width of 1 m. Simulation runs were performed under 6 different loads (2, 10, 20, 100, 200, 400 N).

3.2. Winkler's model

An analogy of the problem with Winkler's idealization of a beam on an elastic foundation was utilized. Winkler's model represents a soil medium as a system of identical but mutually independent, closely spaced, discrete, linearly elastic springs.

This approach was previously used in [5] to describe the take-up bar deflection $y(x)$ in a more proper way than just a simple model of a constantly loaded beam. The following differential equation was used:

$$y(x) \cdot K + \left(\frac{d^4}{d\,x^4} \cdot y(x) \right) \cdot EJ = 0, \tag{1}$$

where K denotes a stiffness of warp yarns, and EJ represents a bending stiffness of the bar. The following solution of Winkler's model differential equation was used to describe the take-up bar deflection $y(x)$:

$$\begin{aligned} y(x) = e^{\beta \cdot x} \cdot (C_1 \cdot \sin(\beta \cdot x) + C_2 \cdot \cos(\beta \cdot x)) + \\ e^{-\beta \cdot x} \cdot (C_3 \cdot \sin(\beta \cdot x) + C_4 \cdot \cos(\beta \cdot x)) + C_5 \cdot x \; + C_6 \,, \end{aligned} \tag{2}$$

where $\beta = \sqrt[4]{\frac{K}{4EJ}}$. By solving a system of linear equations built over appropriate boundary conditions, a set of C_i was obtained. The load applied to the bar was considered along the entire length 2100 mm, unloaded 51 mm ending sections were not taken into account.

Unlike the gap elements in the FEM simulation, the Winkler's model does not consider a release of springs when tension goes to compression. However, for simplification, those transitions were used to determine the loosened warp yarn widths.

3.3. Measurements on the DIFA II machine

In Figure 12, a measuring campaign of the take-up bar deflection is displayed on the DIFA II weaving machine. For the measurements, high-strength polyester binding yarns were used of fineness 550 dtex in a count of 223. All of the different manufactured variants of the bar were measured. Each bar was placed in the operating position, amid the weaving line and drawing off motion. For the purpose of measurements, binding yarns and the bar were placed above the fabric. The following sequence was carried out in order to measure each take-up bar deflection value: the warp beam of binding yarns was rolled back until the control panel of the machine showed desired overall warp tension, supplementary measuring base (yellow duralumin profile in Fig. 12) was slightly pushed against the take-up bar endings, in the middle of the bar the deflection value was read by a digital calliper. The final deflection values were geometrically corrected. The overall warp tension on the machine is sensed by a set of 6 strain gauges supporting the warp yarns under a specific angle.

In the central area of the bar, loosened yarns are visible (Fig. 12), in spite of this, it was not possible to reliably determine and measure widths of loosened yarns, especially for lower loads. This is due to the complexity of the warp system within the weaving machine, fineness and twist of the yarns.

Fig. 12. Illustration from the measurements of the take-up bar deflection

4. Results

For the sake of representation of different profile stiffness, two take-up bar variants, c and d, were chosen and examined. In Figures 13 and 14, results of one simulation run of the numerical model by Siemens NX are shown.

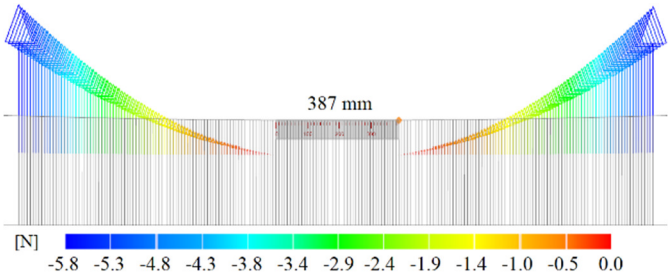

Fig. 13. Reaction force in each yarn along the take-up bar length. The bar type d, load force 400 N, yarns stiffness 420 N·m^{-1}

In Figure 13, a force distribution is depicted among the yarns, where the most outer yarns are loaded by a maximal tensile force of 5.8 N. In the denoted central section of 387 mm, there are 43 unloaded yarns.

In Table 2 are listed unloaded yarns widths obtained by different methods. It is clear that the width of unloaded yarns obtained analytically by the Winkler's model is not sensitive to the applied load; however, it does give a rough insight into this phenomenon.

In the case of FEM simulation, the obtained unloaded widths are smaller compared to analytical solutions. Moreover, with increasing load force the unloaded width decreases. In the case of the bar type c, load force 400 N, and less stiff yarns, there are no loosened yarns.

Table 2. Unloaded yarns width determined by FEM simulation (SIM) and analytically by Winkler's model (WIN)

Load force [N]	Unloaded yarns width [mm]			
	Bar type (c)		Bar type (d)	
	SIM	WIN	SIM	WIN
Yarns tensile stiffness 420 N·m^{-1}				
2	351	448	918	1176
10	351	448	891	1176
20	351	448	891	1176
100	306	448	837	1176
200	162	448	711	1176
400	0	448	387	1176
Yarns tensile stiffness 840 N·m^{-1}				
2	873	1138	1197	1395
10	873	1138	1197	1395
20	873	1138	1197	1395
100	864	1138	1170	1395
200	837	1138	1107	1395
400	747	1138	963	1395

Overall, for both methods and the same yarns, the higher the bar bending stiffness, the smaller the unloaded yarn width. Additionally, for both methods and the same bar stiffness, the higher the yarn tensile stiffness, the higher unloaded yarn width.

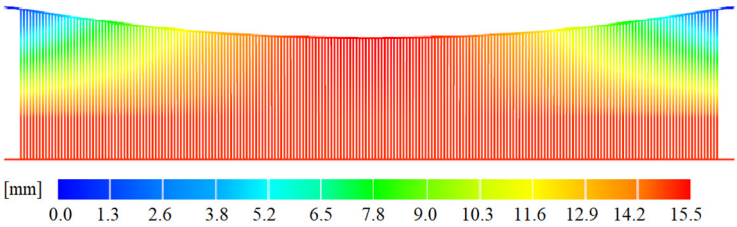

Fig. 14. Deflection of the numerical model's components, upper the take-up bar, lower the auxiliary beam, connected with warp yarns. The bar type d, load force 400 N, yarns stiffness 420 N·m^{-1}

The loading of the take-up bar was analysed for all designs and forces. It is obvious that maximal stress is much lower compared to the strength of material. As an example, in Figure 15, the von Mises stress is shown for the bar type d, with loading force 400 N and yarn stiffness 420 N·m^{-1}. The maximal stress nearly reached 24 MPa. This is about 10 % of the material ultimate strength.

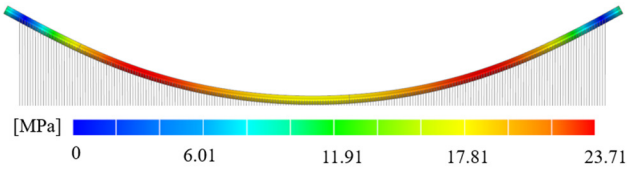

Fig. 15. Von Mises stress of the take-up bar type d, load force 400 N, yarns stiffness 420 N·m^{-1}

Additionally, the simulation run with doubled bar bending stiffness of the bar type c was carried out (Fig. 16). There were no loosened yarns in any applied load, and maximal bar deflection under 400 N load was 10.03 mm compared to 12.58 mm of the bar type c. Nevertheless, a bar design with this bending stiffness would not be possible to fit in the current machine configuration.

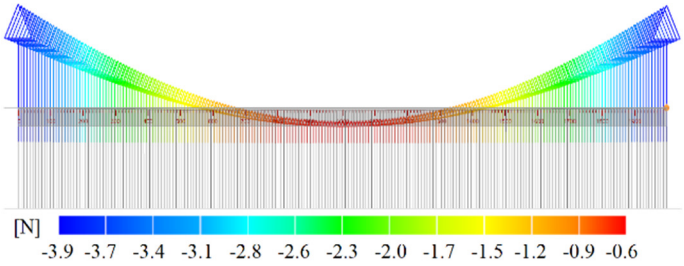

Fig. 16. Reaction force in each yarn along the take-up bar length. The theoretical bar with doubled bending stiffness of the bar type c. Load force 400 N, yarns stiffness 420 N·m^{-1}

In Figure 17 are visualised take-up bars' deflections obtained by different methods. The simulated and calculated results of the bars' deflections are in a load force range from 2 to 400 N, while measured in the range from 100 to 480 N. Deflections under smaller load forces were difficult to measure on the machine by a digital calliper.

There is a good fit in the middle load forces of both theoretical methods with measured deflections for both bar types (c and d). For higher loads, the measured deflections are slightly higher. Overall, measured deflections of the bar type c are about one third lower than of the bar type d. Under the maximal load force of 480 N, the measured deflection of the bar type c is 15.74 mm; this is 29 % better than the deflection of the bar type d 22.30 mm.

For both bars, there is a noticeable decline of FEM calculated deflections under higher load forces compared to the measured ones. It is more prominent for the less stiff bar. It might be related to the boundary conditions of the simulation model, where in the bar attachments only rotation is allowed, with no displacement. However, in the magnetic bar attachments, a displacement might occur. Contrary to that, in terms of deflection, Winkler's model behaves linearly.

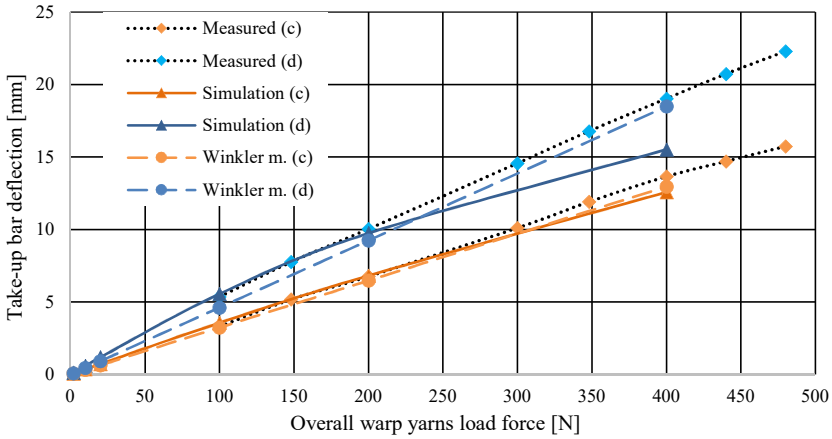

Fig. 17. Take-up bars' deflections determined by different methods

Based on the results of this study, and also by considering other aspects and evolving other bars' specific elements and properties not covered in this study, new take-up bars of proposed designs were manufactured, deeply examined, and tested. In Figure 18, different newly manufactured take-up bar types are displayed. Nevertheless, from many points of view, the promising design of the bar type b (Fig. 2b) could not be realized because of rather short stainless steel sheet metal bends, which are impossible to create with basic tools on a press brake. This could be overcome with a single purpose tool, however, it would be very costly considering the produced amount.

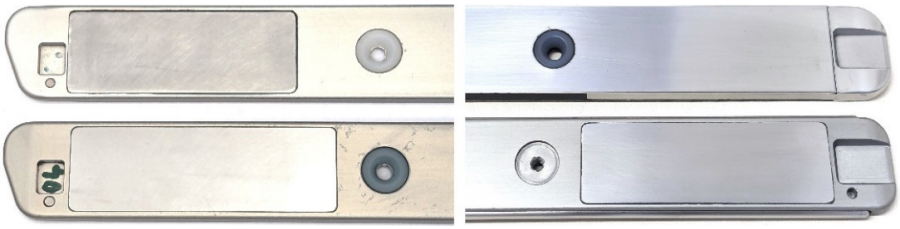

Fig. 18. Take-up bar front endings (left upper type d, left lower type e) and rear endings (right upper type c, right lower type f)

5. Conclusions

This study has brought a deeper understanding of the behaviour of the system of the take-up bar – warp yarns within the DIFA II weaving machine. Properties of the drop-stitch fabric produced are decisive. Assuming the DIFA II weaving machine can process a different amount of binding yarns with a variety of mechanical properties, in regard to the results, it is obvious that the higher the take-up bar bending stiffness, the lower the width of the loosened yarns and the lower bar deflection.

On the other hand, the higher yarn tensile stiffness, or the yarns' count, the wider loosened yarn width.

When the take-up bar type d is considered as an intermediate version to the new type c, there is a noticeable decrease of loosened yarn widths (it varies with force load, yarn stiffness, and method used) up to no loosened yarns in the case of FEM simulation of 400 N load force, yarn stiffness of 420 $N \cdot m^{-1}$.

In terms of measured deflection, the bar type c performed roughly by one third better than the bar type d. Overall, there is a good fit of the measured bar deflection to the deflection determined by both theoretical methods, FEM simulated and analytically determined by Winkler's model.

The progression of the take-up bar design is a trade-off between many factors, mainly the production technology and commonly available materials. Except the bar type b, all the proposed take-up bars were manufactured and examined.

It was found that by increasing the bar bending stiffness to the maximal reasonable values in given cross-sectional dimensions, for certain warp yarns there is still an occurrence of loosened yarns in the central take-up bar section, potentially causing quality issues on the final 3D fabric. In general, the deflection itself might be problematic. There is a proposal for further research and development where the take-up bar could be additionally attached in the middle, the maximal deflection would then decrease significantly (roughly 38 fold). However, other emerged issues would have to be overcome.

Acknowledgment

This work has been elaborated in the framework of project TM02000031 "The Production Technology Performance Increase and Distance Fabrics Utility Properties Extension for New Applications".

References

[1] Zhao, Y., et al. (2023). Compressive properties investigation of "stress transformer" based on high-distance woven spacer fabric design. *Journal of Industrial Textiles*, *53*. DOI: 10.1177/15280837231164785.

[2] Teng, Y.-S., et al. (2011). Weaving Machines and Three-Dimensional Woven Fabrics, US Pat. 2011/0132488 A1 and US 8 015 999 B2, 09/13/2011.

[3] Halbach, K. (1980). Design of permanent multipole magnets with oriented rare earth cobalt material. *Nuclear Instruments and Methods*, *169*(1), 1-10. DOI: 10.1016/0029-554X(80)90094-4.

[4] Aydin, E., et al. (2020). Optimization of elastic springs supports for cantilever beams. *Structural and Multidisciplinary Optimization*, *62*. DOI: 10.1007/s00158-019-02469-3.

[5] Žák, J. (2016). Dimensioning of the take-up bar on a weaving loom using Winkler's model of soil. *Computational Mechanics 2016*, 151. Plzeň, University of West Bohemia, ISBN: 978-80-261-0647-0.